Clinical Cancer Research

Loss of ARID1A in Tumor Cells Renders Selective Vulnerability to Combined Ionizing Radiation and PARP Inhibitor Therapy

Youngran Park[1,2], M. Herman Chui[1,2], Yohan Suryo Rahmanto[1,2], Zheng-Cheng Yu[1,2], Raghavendra A. Shamanna[3], Marina A. Bellani[3], Stephanie Gaillard[4,5,2], Ayse Ayhan[1,6,7], Akila Viswanathan[4,8,2], Michael M. Seidman[3], Sonia Franco[5], Anthony K.L. Leung[4,2,9], Vilhelm A. Bohr[3], Ie-Ming Shih[2,10], and Tian-Li Wang[1,2,10]

Abstract

Purpose: Somatic inactivating mutations in ARID1A, a component of the SWI/SNF chromatin remodeling complex, are detected in various types of human malignancies. Loss of ARID1A compromises DNA damage repair. The induced DNA damage burden may increase reliance on PARP-dependent DNA repair of cancer cells to maintain genome integrity and render susceptibility to PARP inhibitor therapy.

Experimental Design: Isogenic ARID1A$^{-/-}$ and wild-type cell lines were used for assessing DNA damage response, DNA compactness, and profiling global serine/threonine phosphoproteomic *in vivo*. A panel of inhibitors targeting DNA repair pathways was screened for a synergistic antitumor effect with irradiation in ARID1A$^{-/-}$ tumors.

Results: ARID1A-deficient endometrial cells exhibit sustained levels in DNA damage response, a result further supported by *in vivo* phosphoproteomic analysis. Our results show that ARID1A is essential for establishing an open chromatin state upon DNA damage, a process required for recruitment of 53BP1 and RIF1, key mediators of nonhomologous end-joining (NHEJ) machinery, to DNA lesions. The inability of ARID1A$^{-/-}$ cells to mount NHEJ repair results in a partial cytotoxic response to radiation. Small-molecule compound screens revealed that PARP inhibitors act synergistically with radiation to potentiate cytotoxicity in ARID1A$^{-/-}$ cells. Combination treatment with low-dose radiation and olaparib greatly improved antitumor efficacy, resulting in long-term remission in mice bearing ARID1A-deficient tumors.

Conclusions: ARID1A-deficient cells acquire high sensitivity to PARP inhibition after exposure to exogenously induced DNA breaks such as ionizing radiation. Our findings suggest a novel biologically informed strategy for treating ARID1A-deficient malignancies.

Introduction

Altered chromatin structure, due to somatic mutations or epigenetic alterations of genes involved in chromatin remodeling, is a major contributor to tumor development (1). SWI/SNF chromatin remodeling complexes are an important class of epigenetic modulators, which regulate a plethora of basic biological functions including DNA replication, transcription, and DNA repair by remodeling chromatin configuration. Loss-of-function mutations in SWI/SNF genes have been identified in many types of human cancer, and an important example is the AT-rich interactive domain 1A (ARID1A) gene, which is the most frequently mutated subunit in the SWI/SNF chromatin remodeling complex (2–5). ARID1A mutations are frequently detected in endometrium-derived cancers including approximately 50% of ovarian clear cell carcinomas, approximately 35% of uterine endometrioid carcinomas, and approximately 30% of ovarian endometrioid carcinomas (2, 5–7). Mutations in ARID1A have also been reported in stomach, bladder, pancreas, and hepatocellular carcinomas among others (8–12). ARID1A is a tumor suppressor, and functions as a cell-cycle checkpoint protein (3). Genetically engineered mice with ARID1A deletions in their ovarian surface epithelium are known to develop ovarian carcinomas in a background of PTEN inactivation or PIK3CA activation (13, 14).

[1]Department of Pathology, Johns Hopkins University School of Medicine, Baltimore, Maryland. [2]Sidney Kimmel Comprehensive Cancer Center, Johns Hopkins University School of Medicine, Baltimore, Maryland. [3]Laboratory of Molecular Gerontology, National Institute on Aging, NIH, Baltimore, Maryland. [4]Department of Oncology, Johns Hopkins University School of Medicine, Baltimore, Maryland. [5]Department of Gynecology/Obstetrics, Johns Hopkins University School of Medicine, Baltimore, Maryland. [6]Department of Pathology, Seirei Mikatahara General Hospital, Hamamatsu, Japan. [7]Hiroshima University School of Medicine, Hiroshima, Japan. [8]Department of Radiation Oncology and Molecular Radiation Sciences, Johns Hopkins University School of Medicine, Baltimore, Maryland. [9]Department of Biochemistry and Molecular Biology, Bloomberg School of Public Health, Johns Hopkins University, Baltimore, Maryland. [10]Richard W. TeLinde Gynecologic Pathology Research Program, Johns Hopkins University School of Medicine, Baltimore, Maryland.

Note: Supplementary data for this article are available at Clinical Cancer Research Online (http://clincancerres.aacrjournals.org/).

Corresponding Authors: Ie-Ming Shih, Johns Hopkins Medical Institutions, 1550 Orleans Street, CRB-2, 305, Baltimore, MD 21231. Phone: 410-502-7774; Fax: 410-502-7943; E-mail: ishih@jhmi.edu; and Tian-Li Wang, tlw@jhmi.edu

Clin Cancer Res 2019;25:5584–94

doi: 10.1158/1078-0432.CCR-18-4222

Translational Relevance

The role of PARP inhibitors beyond the treatment of homologous recombination–deficient cancers remains to be explored. ARID1A-deficient tumors, which are characterized by an attenuated capacity to carry out nonhomologous end-joining DNA repair, are only partially sensitive to PARP inhibitors. Here, we provide evidence that ARID1A-deficient tumors can become highly sensitive to PARP inhibitors following treatments, such as irradiation, that exogenously induce DNA breaks. Our findings provide preclinical evidence supporting a novel strategy for targeted treatment of ARID1A-deficient cancers and provide insight into the contribution of ARID1A in mediating DNA repair and replication.

The finding of frequent ARID1A mutations in endometrium-derived cancers suggests that targeting the ARID1A pathway as an anticancer intervention has translational potential. However, it has become apparent that targeting tumor suppressor genes such as *TP53* using a standard pharmacologic approach is highly challenging; in contrast, targeting gain-of-function oncogenes by pharmacologic and antibody interventions has proven to be more promising. Nonetheless, loss-of-function mutations in tumor suppressors may result in acquisition of dependence of cancer cells on alternative compensatory pathway(s) or downstream molecular effector(s). This unique feature of loss-of-function mutations in tumor suppressor genes offers opportunities for targeting cancer cells by disrupting compensatory or alternative pathway(s) (15). A well-known example is the sensitivity of tumor cells with BRCA-inactivation to PARP inhibition, a consequence of their deficiency on homologous repair (HR; refs. 16, 17).

To extend this strategy to ARID1A$^{-/-}$ tumors, we sought first to understand the impact of inactivation of ARID1A or other SWI/SNF chromatin remodeling proteins in DNA damage repair pathways (18–20). In mammalian cells, DNA double-strand breaks (DSB) are predominantly repaired by the NHEJ and HR pathways, each of which harness a unique set of molecular players. The balance between both pathways is essential for genome stability, and disturbance of the balance often leads to disease, including cancer. SWI/SNF chromatin remodeling has been reported to participate in the early phase (before strand intrusion phase) of DSB repair through rapid localization to the DSB sites, clearing local nucleosome occupancy, and physically facilitating recruitment of DNA repair enzymes and other modulators to the vicinity of DSBs (18–20). Thus, loss of ARID1A may disturb the balance of HR/NHEJ DNA repair efficacy and may render cells susceptible to specific genotoxic treatment. Indeed, two studies reported the involvement of ARID1A in NHEJ- and HR-mediated DSB repair, respectively (21, 22). However, ARID1A inactivation–induced negative regulation of both NHEJ and HR repair pathways remains of interest, and has yet to be fully elucidated (23). It also remains to be determined which DNA repair mechanism or molecular pathway is employed by ARID1A-deficient tumors for survival and maintenance of DNA integrity in the face of endogenous stress and environmental challenges that result in DNA damage.

In this study, we first established that ARID1A deficiency led to a functional compromise in NHEJ repair and, to a lesser degree, in HR or alt-NHEJ. Similar to cells with NHEJ deficiency, ARID1A-deficient cells were partially sensitive to radiation-induced DNA damage, likely due to sufficient HR DNA repair activity. Using a synthetic lethal screen to identify drugs affecting DNA repair that might act in concert with irradiation in ARID1A-deficient tumor cells, we identified PARP inhibitor as a strong candidate. Applying this treatment approach in animal models, we were able to induce long-term remission in ARID1A-deficient tumors, which persisted after completion of the treatment, whereas the same treatment was not effective in tumors with intact ARID1A function. Our findings indicate that disturbance of the DNA repair balance associated with ARID1A deficiency can be exploited to develop highly specific and potent anticancer treatments.

Materials and Methods

Animal studies and tumor xenografts

All animal-related procedures were approved by the Johns Hopkins University Animal Care and Use Committee. PAX8-rtTA/TetO-Cre mouse strains were acquired from Dr. Ronny Drapkin (13, 24). Arid1a$^{flox/flox}$ mice were generated as described previously (13, 24). For xenograft assays, 2×10^6 cells were injected subcutaneously with Matrigel (v/v; BD Biosciences) into flanks of athymic *nu/nu* mice. Once the tumor volume reached approximately 100 mm^3 (approximately 10–14 days), mice were randomized into four groups for further analysis.

Human tissue samples

Archived formalin-fixed and paraffin-embedded human tissues were provided by Seirei Mikatahara General Hospital (Shizuoka, Japan). All specimens were deidentified and the study was approved by local ethical committee (IRB No.14–46; 2014/12/15) for a waiver of informed consent of the subjects.

Cell lines

The immortalized normal human endometrial cell line, hEM3, previously established in our team was used for this study (25). Knockout of ARID1A was performed as described previously (25). Two pairs of isogenic cell lines, HCT116 and MCF10A (ARID1A$^{+/+}$, ARID1A$^{-/-}$), were purchased from Horizon Discovery Ltd. We used a previously established ARID1A-Tet-on OVISE cell line, which originally lacks ARID1A expression due to inactivating mutations and reexpresses ARID1A upon tetracycline induction (3). Other cancer cell lines (TOV21G1, RMG1, HEC151, and ECC1) were grown as described previously (25).

Laser microirradiation assay

Cells were seeded in a Nunc glass-bottom dish (Thermo Fisher Scientific). After 5-minute incubation with 2 μmol/L Hoechst (Thermo Fisher Scientific), cells were mounted on a preheated (37°C) stage of a Zeiss LSM 710 confocal microscope equipped with a 405-nm laser source. To induce localized DSBs, the laser setting was set to 100% power output with four laser iterations. Image analysis was performed using Zeiss Zen 2010 software.

Statistical analyses

Mann–Whitney test (two-tailed) was used to calculate the statistical significance between two experimental groups. A

combination index was calculated as described previously (26), and synergistic drug interactions were analyzed by the method developed by Chou and Talalay (27). Two-way ANOVA with Bonferroni correction was used to calculate the statistical significance in experiments (Fig. 2C–E; Supplementary Fig. S4). Statistical analyses were performed using GraphPad Prism 7 software. All results are expressed as means ± SEM. Two-sided $P \leq 0.05$ was considered significant.

Other methods can be found in Supplementary Materials.

Results

ARID1A deficiency is associated with a sustained DNA damage response and DSBs

To study the role of ARID1A in DNA damage, we first quantified DNA damage and the damage response in complex atypical hyperplasia (CAH) of endometrium, which exhibited focal and heterogeneous loss of ARID1A in the same tissue sections (left, Fig. 1A). IHC analysis showed more intense phospho-H2AX (S139, γH2AX) immunoreactivity in ARID1A-negative tumor

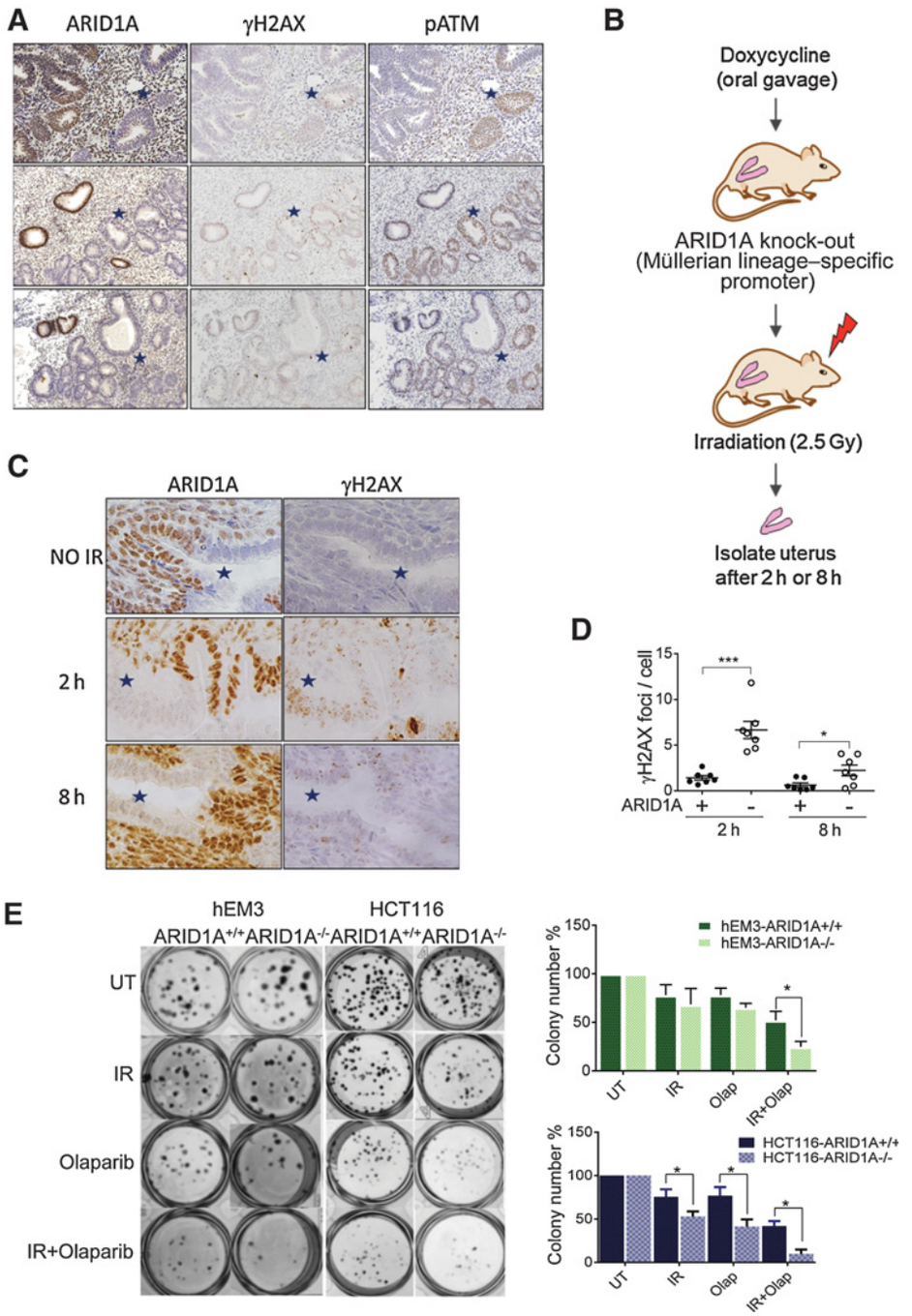

Figure 1.
ARID1A deficiency results in sustained DSBs and sensitizes cells to irradiation. **A,** IHC staining patterns of ARID1A, γH2AX, and phosphorylated-ATM (s1981) in complex atypical hyperplasia (CAH) of endometrium. ARID1A-loss of expression areas are marked with blue stars. Representative images are shown. **B,** Schematic illustration of the experimental procedure. **C,** IHC staining of ARID1A and γH2AX in endometrial tissue of ARID1A$^{flox/flox}$ mice. Mice were treated with doxycycline for 1 week to induce deletion of ARID1A, and were sacrificed for analysis at the indicated time points after irradiation (2.5 Gy). ARID1A-loss areas are marked with blue stars. Representative images are shown. **D,** Quantitation of γH2AX foci per endometrial epithelial cell. Data are presented as mean ± SEM; more than 500 cells were analyzed per group. Mann–Whitney test (two-tailed) was used to calculate significance; *, $P < 0.05$; ***, $P < 0.001$. **E,** Clonogenic formation visualized by crystal violet staining on day 7 postirradiation. Colony numbers were quantified and plotted (right). Data are presented as mean ± SEM, $n = 6$; *, $P < 0.05$.

areas, compared with adjacent areas with ARID1A expression (middle, Fig. 1A; Supplementary Fig. S1). To confirm that increased γH2AX staining reflected DSBs, we also stained tissues with phosphorylated ATM (S1981), a marker of an activated DNA damage response. We observed concordance between pATM and γH2AX staining (right, Fig. 1A), implying that unrepaired DSBs were more prevalent in ARID1A-deficient epithelial cells.

Although previous studies implicate chromatin remodeling proteins such as ARID1A in DNA repair, such findings have rarely been validated *in vivo*. To functionally establish the *in vivo* role of ARID1A in DSB repair, we assessed the status of DNA damage using a genetically engineered mouse model with conditional deletion of *ARID1A*. This model was established by crossing ARID1A$^{flox/flox}$ mice with PAX8-Cre mice carrying doxycycline-inducible Cre recombinase under control of the Pax8 promoter (Fig. 1B). Pax8 is a transcription factor expressed in Mullerian epithelial cells lining the gynecologic tract, including endometrial epithelial cells; thus, doxycycline administration caused Pax8-driven, endometrial epithelium–specific deletion of ARID1A. In early stages of doxycycline administration, we observed a heterogeneous loss of ARID1A in murine uterine epithelium, shown by stretches of endometrial epithelium with ARID1A loss (stars in left panels, Fig. 1C) alternating with stretches of ARID1A-expressing epithelium (Fig. 1C). This provided an opportunity to directly compare DNA damage in ARID1A-expressing and nonexpressing epithelium from the same animals. Whole-animal irradiation (2.5 Gy) was used to induce DSBs. IHC staining revealed more prominent γH2AX punctate foci in ARID1A$^{-/-}$ cells at 2 hours and 8 hours postirradiation compared with ARID1A-intact cells (right, Fig. 1C). Quantification of γH2AX foci per cell indicated that the increase in punctate foci in ARID1A$^{-/-}$ cells was significant (Fig. 1D).

To further assess the mechanistic role of ARID1A in DSB repair, we deleted ARID1A in an immortalized endometrial epithelial cell line, hEM3, using CRISPR/Cas9. Consistent with *in vivo* observations, irradiation resulted in higher levels of γH2AX in hEM3-ARID1A$^{-/-}$ than in hEM3-ARID1A$^{+/+}$ cells at all timepoints examined (top, Supplementary Fig. S2A). We verified these results in parental hEM3 cells following siRNA-mediated silencing of ARID1A (bottom, Supplementary Fig. S2A). Introduction of ARID1A in Tet-on OVISE diminished γH2AX levels (Supplementary Fig. S2B). Results of a comet assay showed that ionizing radiation–induced DNA DSBs were exacerbated by siRNA-mediated ARID1A silencing in parental hEM3 cells, and were rescued by ARID1A reexpression in ARID1A-mutated OVISE cells (Supplementary Fig. S2C and S2D).

We next performed a clonogenic assay to determine whether ARID1A-deficient cells were more sensitive to radiation-induced DNA damage. After irradiation, we observed a modest decrease in survival of HCT116-ARID1A$^{-/-}$ cells; however, we could not observe a different clonogenic survival after irradiation in hEM-ARID1A$^{+/+}$ and ARID1A$^{-/-}$ cells (Fig. 1E). These results suggest that increased DNA damage in ARID1A-deficient cells could be rescued by a compensatory survival pathway, and suggest that an additional treatment combined with irradiation would be required for killing ARID1A-deficient cells.

DNA repair and cell-cycle regulatory proteins associated with ARID1A deficiency identified by global *in vivo* phosphoproteomic profiling

To explore the underlying mechanism of increased DNA damage signals in ARID1A-depleted cells, we performed global *in vivo* serine/threonine phosphoproteomic profiling as an unbiased approach to interrogate differential cellular responses to irradiation between ARID1A$^{-/-}$ and ARID1A$^{+/+}$ tumor xenografts (Supplementary Table S1). Network analysis showed enrichment of proteins with altered phosphorylation involved in DNA replication and repair, including ATM, 53BP1, TOP2A, and TOP2B, in ARID1A$^{-/-}$ tumors (Supplementary Fig. S3A). The finding of enriched pATM expression by phosphoproteomic profiling orthogonally validated our immunostaining data. Using ingenuity pathway analysis (IPA), we found enriched pathways including NHEJ and base excision repair (BER) DNA repair pathways involving XRCC1, XRCC4, ATM, and PRIM1, as well as cell-cycle control of chromosomal replication pathway involving TOP2A, TOP2B, and CDC7 (Supplementary Fig. S3B). Collectively, our data provide new evidence of ARID1A in DSB, replication, and repair regulation. The data also support a view that defects in these pathways resulting from ARID1A loss led to a prolonged DNA damage response and persistence of DSBs after DNA damage insults.

ARID1A-dependent chromatin regulation and recruitment of NHEJ repair proteins

To determine whether ARID1A was required for NHEJ and/or HR, we monitored both repair mechanisms simultaneously (Fig. 2A; ref. 28). A significant decrease in NHEJ activity was observed in ARID1A$^{-/-}$ cells. HR activity was also slightly decreased in ARID1A$^{-/-}$ cells, although precise quantitation of HR was difficult due to the low level of HR even in the setting of ARID1A-intact cells. The impact of ARID1A loss on NHEJ appears to be of biological significance, as a high proportion of cells rely on this pathway. We further characterized the impact of ARID1A in alt-NHEJ, a NHEJ subpathway (29, 30). Knockdown of CtIP (effector) and 53BP1 (suppressor) served as controls. We found that alt-NHEJ was also decreased in ARID1A-depleted cells (Fig. 2B). Thus, the data indicate that ARID1A deficiency causes impairment of DSB repairs, with NHEJ repair pathway being most significantly compromised.

Because the activity of NHEJ and HR DNA repair pathways is cell-cycle dependent (31), we asked whether ARID1A-deletion caused cell-cycle alterations, which may indirectly affect DNA repair. Cell-cycle analysis of hEM3 isogenic cell lines indicated that ARID1A$^{-/-}$ cells displayed reduced S and G_2–M fractions compared with ARID1A$^{+/+}$ cells (Supplementary Fig. S4). This result is consistent with that observed in a pair of isogeneic HCT116 cell lines (22). Because HR occurs primarily during S and G_2–M phases, we postulate that reduced HR observed in ARID1A-deficient cells can likely be attributed to attenuation in S and G_2–M phases.

To determine whether an ARID1A-dependent process is required for recruitment of NHEJ repair proteins, we monitored recruitment of 53BP1 to DNA damage lesions induced by laser microirradiation. We found a significant delay in the recruitment of this key NHEJ repair factor to sites of laser-induced DNA damage in ARID1A-deficient cells (Fig. 2C). Restoration of ARID1A expression in ARID1A-deficient cells partially restored 53BP1 recruitment efficiency (Fig. 2D). Similar results were observed for RIF1, another crucial component of the NHEJ repair pathway acting downstream of 53BP1 (Fig. 2E). There was no evidence of reciprocal regulation of ARID1A recruitment to DSBs by 53BP1. Knockdown or knockout of ARID1A in mammalian cells did not affect 53BP1 recruitment to DSBs induced by

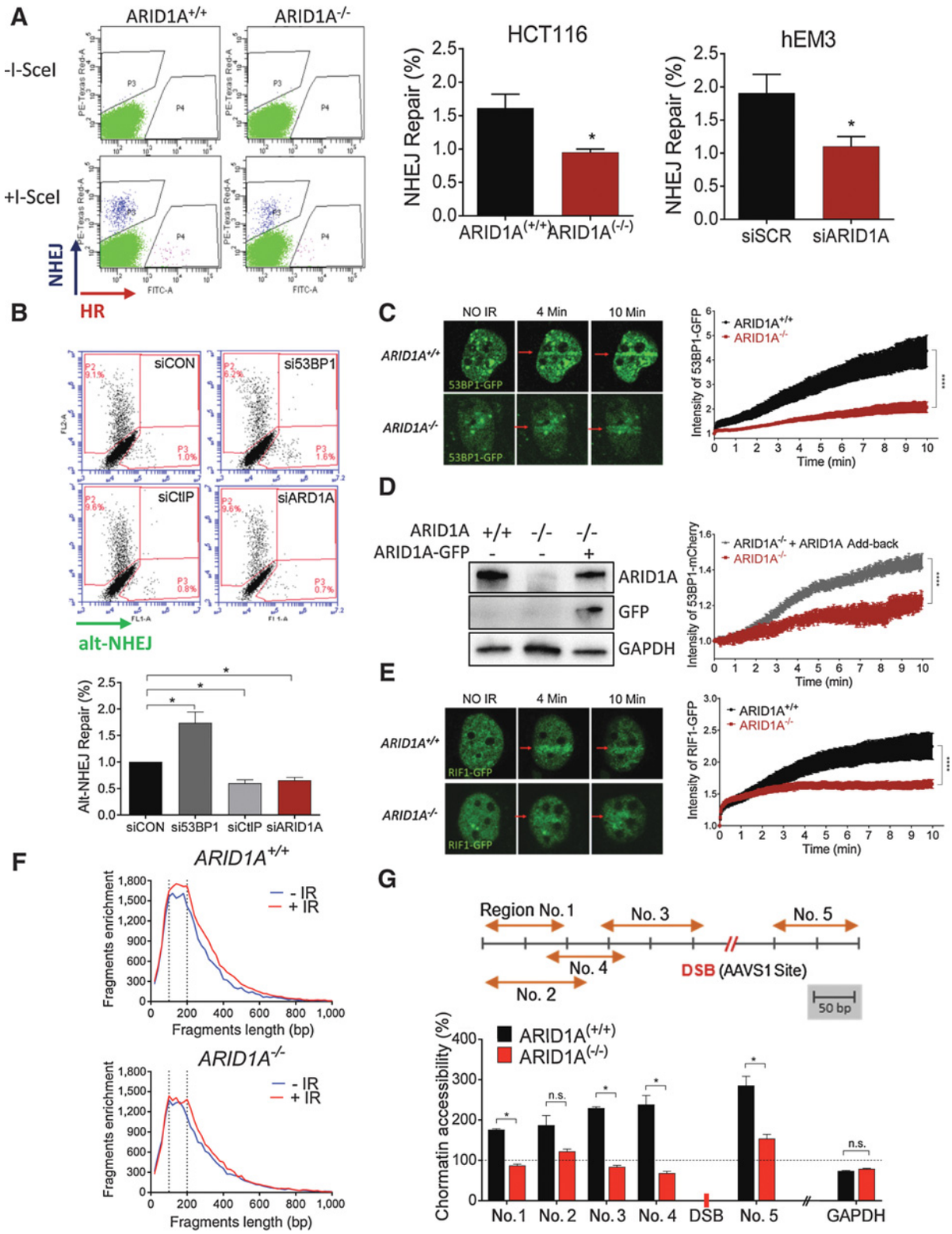

microirradiation (Supplementary Fig. S5). Collectively, our results show that ARID1A deficiency compromises NHEJ repair by preventing the recruitment of key NHEJ proteins, including 53BP1 and RIF1, to DSB sites.

Because SWI/SNF complexes function as master regulators of chromatin structure, we hypothesized that regulation of the chromatin landscape by ARID1A is a key step in response to DSBs. To assess genome-wide chromatin configuration (openness vs. compactness), we performed ATAC-seq in ARID1A$^{+/+}$ and ARID1A$^{-/-}$ cells before, and 1 hour after, irradiation (Fig. 2F). Enrichment of 146 bp DNA fragments indicates an increased open chromatin state because these fragments correspond to mononucleosome occupancy. As compared with ARID1A$^{-/-}$ cells, a larger 146 bp DNA peak was observed in ARID1A$^{+/+}$ cells after irradiation, implicating a functional role of ARID1A in modulating the global chromatin state in response to ionizing radiation. We introduced site-specific DSBs near the AAVS1 locus (chromosome 19) and the GAPDH locus (chromosome 12) in ARID1A$^{+/+}$ and ARID1A$^{-/-}$ cells using CRISPR/Cas9, and evaluated chromatin accessibility near the introduced DSBs (described in Supplementary Materials). As expected, we observed increased chromatin accessibility at genomic regions proximal to the AAVS1 locus in ARID1A$^{+/+}$ cells compared with ARID1A$^{-/-}$ cells (Fig. 2G). We did not observe significant differences in chromatin accessibility at genomic regions near GAPDH in ARID1A$^{+/+}$ cells compared with ARID1A$^{-/-}$ cells (Fig. 2G). On the basis of these data, we conclude that ARID1A-dependent alteration in chromatin configuration, which facilitates the recruitment of key effectors of the DNA repair machinery to the damaged sites, is a prerequisite step for initiating DSB repair.

Synergistic cytotoxicity of PARP inhibition and irradiation in ARID1A-deficient cells

Because ARID1A-deficient cells were only marginally more radiosensitive than ARID1A-intact cells, we sought to identify an approach to enhance the therapeutic index. Because platinum-based chemotherapy (for example, carboplatin), is routinely used for treatment of ovarian and endometrial carcinomas, and has been shown to increase sensitivity to radiotherapy (32, 33), we tested the sensitivity of ARID1A-deficient cells to carboplatin, either as a single agent or in combination with radiation. Clonogenic assays were performed on isogenic pairs of ARID1A$^{+/+}$ and ARID1A$^{-/-}$ cells derived from hEM3 and HCT116 parental cell lines. Although hEM3-ARID1A$^{-/-}$ cells were slightly more sensitive to carboplatin than ARID1A$^{+/+}$ cells, differences were less apparent in the HCT116 isogenic model. For both cell types, carboplatin combined with irradiation did not result in appreciable improvements over single-agent treatment (Supplementary Fig. S6A and S6B). This negative result prompted us to screen a panel of additional chemotherapeutic drugs and inhibitors of DNA repair and of epigenetic regulators (Fig. 3A; Supplementary Fig. S7). Among these drugs screened, the PARP inhibitor, olaparib, emerged as the most potent and specific radiosensitizer for ARID1A$^{-/-}$ cells (Fig. 3A). ATR inhibitor, AZD-6783, also enhanced potency of radiotherapy for ARID1A$^{-/-}$ cells. PIK-587, a dual PI3K and mTOR kinase inhibitor, potently inhibited cell growth irrespective of ARID1A deletion status (Supplementary Fig. S7). Next, we tested the efficacy of combining PARP inhibitor and irradiation in a 3D culture system on both HCT116 and hEM3 pairs of isogenic cell lines. In these experiments, we observed synergistic cytotoxicity in ARID1A$^{-/-}$ cells (Fig. 3B). The increased sensitivity to ionizing radiation plus PARP inhibitor was further verified in clonogenic cell survival analysis in both hEM3 and HCT116 isogenic cell lines (Fig. 1E).

To gain molecular insight into the synergistic effects, we compared PARP activity between ARID1A$^{-/-}$ and ARID1A$^{+/+}$ cells. We observed elevated basal levels of PolyADP-ribosylation (PARylation) in ARID1A$^{-/-}$ cells (Fig. 3C). This result was confirmed by gene silencing using two different siRNAs (Fig. 3D). Because PARP-mediated PARylation occurs via consumption of NAD^+, the relative level of NAD^+ (NAD/NADH ratio) is another indicator of cellular PARP activity. We found that the NAD/NADH ratio was reduced in hEM3 cells after ARID1A knockdown, confirming increased PARP activity in ARID1A-deficient cells (Fig. 3D). The extent of DNA breaks resulting from single or combined irradiation and PARP inhibitor exposure was assessed by measuring the levels of γH2AX (Fig. 3E). We found that combining PARP inhibition with irradiation led to significant increases in γH2AX levels in ARID1A$^{-/-}$ cells but not in isogenic ARID1A$^{+/+}$ cells (Fig. 3E).

PARP inhibitors are thought to compromise DNA damage repair through two major mechanisms. First, they cause "PARP-trapping" by preventing PARP dissociation from DNA. Another mechanism is through persistence of single-strand breaks, which ultimately progress to DSBs during replication. To determine which mechanisms are relevant to our model, we excluded a PARP-trapping effect by RNAi-mediated knockdown of PARP1 in

Figure 2.

ARID1A deficiency suppresses NHEJ-mediated repair of DSBs and chromatin accessibility. **A,** Left, Flow cytometric analysis of TLR expressing HCT116 ARID1A$^{+/+}$ and ARID1A$^{-/-}$ cells performed 72 hours after transduction with the I-Sec/GFP donor lentiviral construct. DSB repair mediated by HR is seen as GFP+, and repair mediated by NHEJ is seen as mCherry+. Right, histograms show quantification of NHEJ repair in both isogenic HCT116 and gEM3 cells. Data are presented as mean ± SEM, $n = 4$. Mann–Whitney test (two-tailed) was used to calculate statistical significance; *, $P < 0.05$. **B,** Flow cytometric analysis of EJ2-expressing U2OS cells after transfection with specific siRNAs. Four days after transfection with I-Sec, alt-NHEJ repair ability, seen as a GFP+ signal, was quantified and plotted. Data are presented as mean ± SEM, $n = 4$; *, $P < 0.05$. **C,** Left, Representative live-cell images of ARID1A$^{+/+}$ and ARID1A$^{-/-}$ cells expressing 53BP1-GFP at the indicated time points after microirradiation (red arrow). Right, Intensity of GFP at irradiated area (yellow box) was measured every 3 seconds and plotted after normalization. Data are presented as mean ± SEM; more than 7 cells were analyzed per group. **D,** Immunoblots showing expression of ARID1A, GFP, and GAPDH. ARID1A$^{-/-}$ cells were cotransfected with 53BP1-mCherry and/or ARID1A-GFP. The intensity of mCherry at the microirradiated sites from the indicated cells was monitored over time. Data are presented as means ± SEM; more than 6 cells were analyzed per group. **E,** Left, Representative live images of cells transfected with RIF1-GFP at the indicated time points after microirradiation (red arrow). Right, Intensity of GFP at irradiated area (yellow box) was measured every 3 seconds and plotted after normalization. Data were plotted as described in **C**; more than 12 cells were analyzed per group. (**C**–**E**) Two-way ANOVA with Bonferroni correction was used to calculate the statistical significance; ***, $P < 0.001$. **F,** ATAC-seq analysis was performed in ARID1A$^{+/+}$ and ARID1A$^{-/-}$ cells before (blue) and 1 hour after (red) irradiation (4 Gy). Fragment size (~146 bp) shown with dotted lines. **G,** Schematic representation of the genomic locus of AAVS1 (chromosome 19) and regions amplified with specific primers (orange arrows). Following localized DSB at the AAVS1 site (red; CRISPR/Cas9–transfected cells), chromatin was isolated from ARID1A$^{+/+}$ and ARID1A$^{-/-}$ cells and was subjected to nuclease digestion or was untreated. Chromatin accessibility at specified regions was calculated and plotted after normalization to no-DSB control (CRISPR/Cas9 control plasmid transfection). GAPDH, which is located on a different chromosome (chromosome 12), was used as a control. Data are presented as mean ± SEM, $n = 4$; *, $P < 0.05$.

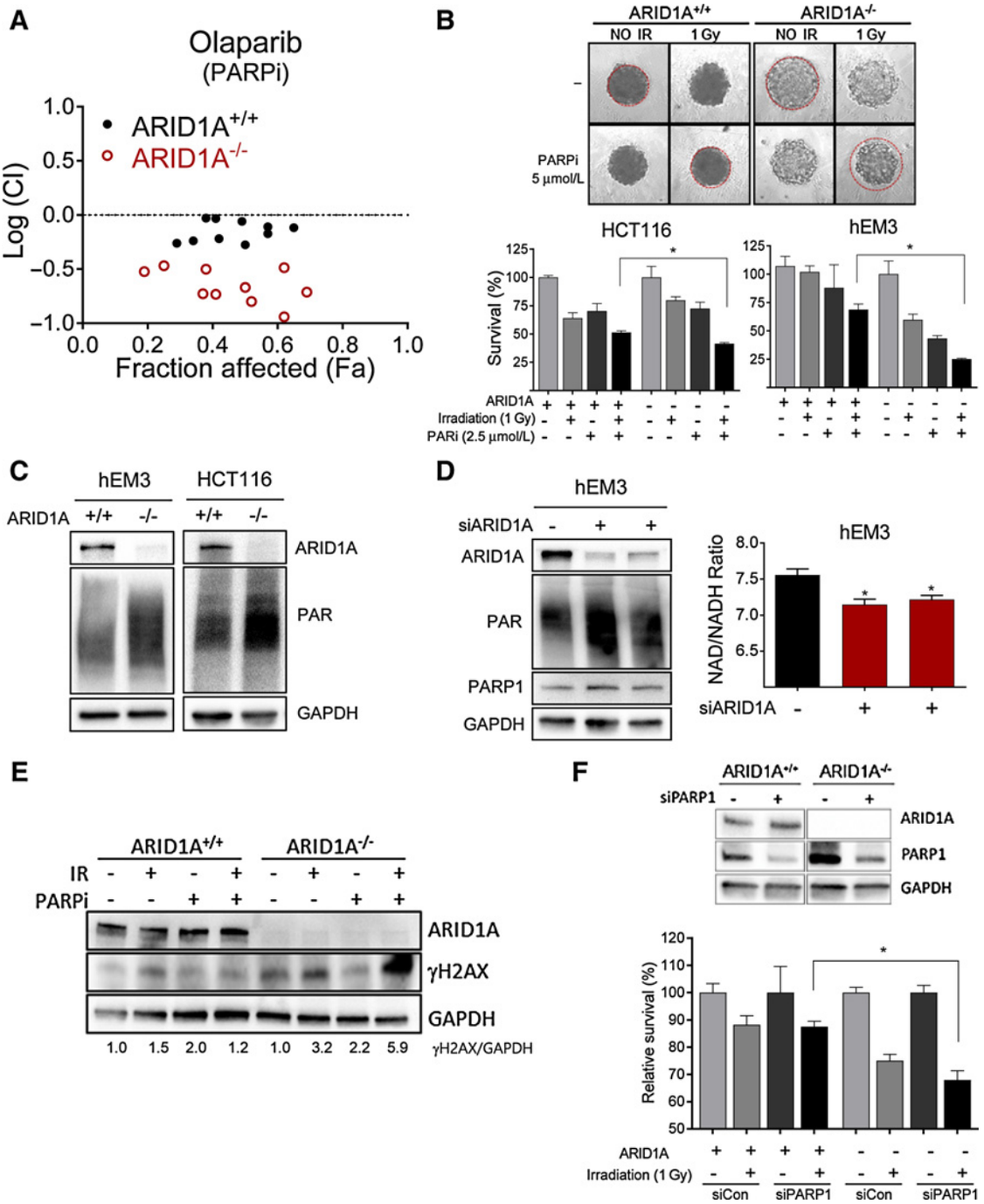

Figure 3.

Synergy between PARP inhibition and radiation in ARID1A-deficient cells. **A,** Logarithmic combination index (CI) plot of irradiation (1–2 Gy) in combination with PARP inhibitor, olaparib, over a range of concentrations in ARID1A$^{+/+}$ and ARID1A$^{-/-}$ cells. The horizontal dashed line at Log (CI) = 0 separates synergy [Log (CI)<0] and antagonism [Log(CI)>0]. **B,** Representative images of 3-D culture spheroids are shown. After treatment as indicated, cell survival was measured and plotted. Data are presented as mean ± SEM, $n = 4$. Mann–Whitney test (two-tailed) was used to calculate the statistical significance between two comparison groups; *, $P < 0.05$. **C,** Immunoblots for ARID1A, PARylation, and GAPDH of extracts from indicated cell lines. **D,** Left, Immunoblots for ARID1A, PARylation, PARP1, and GAPDH of extracts from hEM3 cells transfected with ARID1A siRNA or scramble control siRNAs. Right, NAD/NADH ratio determined in hEM3 cells transfected with ARID1A or control siRNAs. Data are presented as mean ± SEM, $n = 4$; *, $P < 0.05$. **E,** Immunoblots for ARID1A, γH2AX, and GAPDH. The ratio of γH2AX/GAPDH is indicated at the bottom. **F,** (top) Immunoblots showing efficiency of PARP1 silencing by siRNAs. (bottom) Effect of PARP1 knockdown on survival of ARID1A$^{+/+}$ and ARID1A$^{-/-}$ tumor cells in the presence or absence of irradiation. Data are presented as mean ± SEM, $n = 4$; *, $P < 0.05$. Mann–Whitney test (two-tailed).

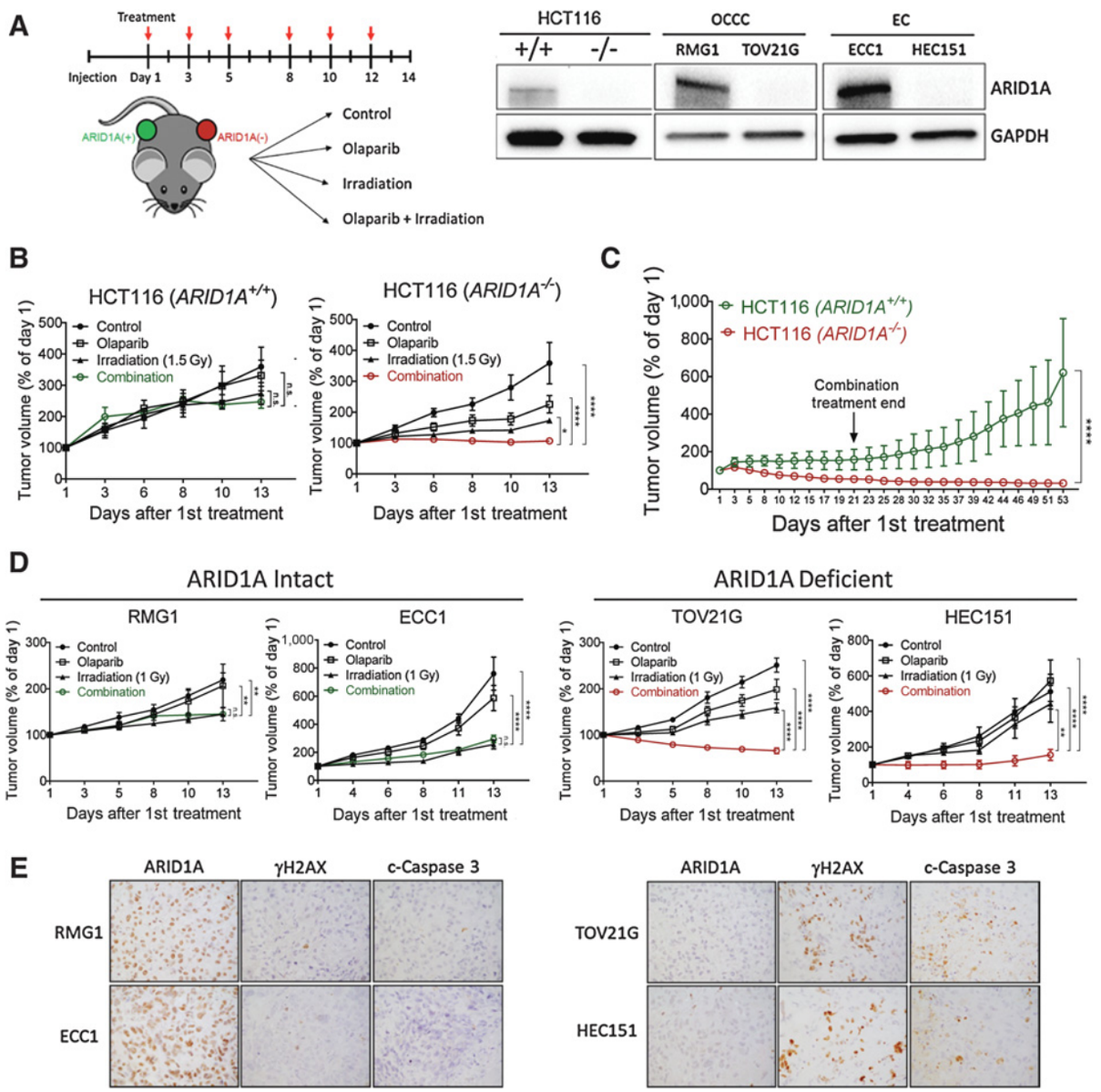

Figure 4.

Combination of PARP inhibitor and ionizing radiation inhibits growth and induces apoptosis in ARID1A-deficient tumor xenografts. **A,** Left, Schematic of treatment regimen in mice. Immunocompromised athymic *nu/nu* mice were inoculated with indicated human tumor cells, and 10–14 days later, mice were randomly stratified into 4 treatment groups. Olaparib (50 mg/kg) and/or irradiation (1–2 Gy) were administrated 3 times per week. Right, Immunoblots performed to assess ARID1A protein expression in each cell line. **B,** Tumor volume of HCT116-ARID1A$^{+/+}$ and ARID1A$^{-/-}$ xenografts monitored for 2 weeks. Data are presented as mean ± SEM, $n = 5$. Mann–Whitney test (two-tailed) was used to calculate the statistical significance between two comparison groups on day 13; *, $P < 0.05$; ****, $P < 0.0001$. **C,** Relative tumor volume measured in mice inoculated with HCT116 cancer cells and treated with olaparib and ionizing radiation (2 Gy) combined therapy for 3 weeks. Tumor growth was monitored until day 53. Data are presented as mean ± SEM, $n = 4$; ****, $P < 0.0001$. **D,** Tumor volume measured in different groups. RMG1 and ECC1 are ARID1A wild-type and express ARID1A protein while TOV21G and HEC151 harbor inactivating mutations and lose ARID1A protein expression. Data are presented as mean ± SEM, $n = 5$; *, $P < 0.05$; **, $P < 0.01$; ***, $P < 0.001$; ****, $P < 0.0001$. **E,** IHC staining of ARID1A, γH2AX, and cleaved caspase-3 in tumor xenografts excised from mice treated with olaparib and ionizing radiation (2 Gy).

hEM3-ARID1A$^{-/-}$ and ARID1A$^{+/+}$ cells. When PARP1 was depleted, ARID1A$^{-/-}$ cells were still more sensitive to irradiation than ARID1A$^{+/+}$ cells (Fig. 3F). These data are consistent with the notion that suppression of PARP1 catalytic activity is the primary mechanism underlying synergy between PARP inhibitor and irradiation.

Combining PARP inhibitor with irradiation is more effective than monotherapy for treating ARID1A-mutated tumors

In light of the observation that irradiation increases PARP inhibitor sensitivity in ARID1A$^{-/-}$ cells, we evaluated this treatment strategy in mice using isogenic HCT116 cell lines that differed only in ARID1A status (right, Fig. 4A). Tumor volumes

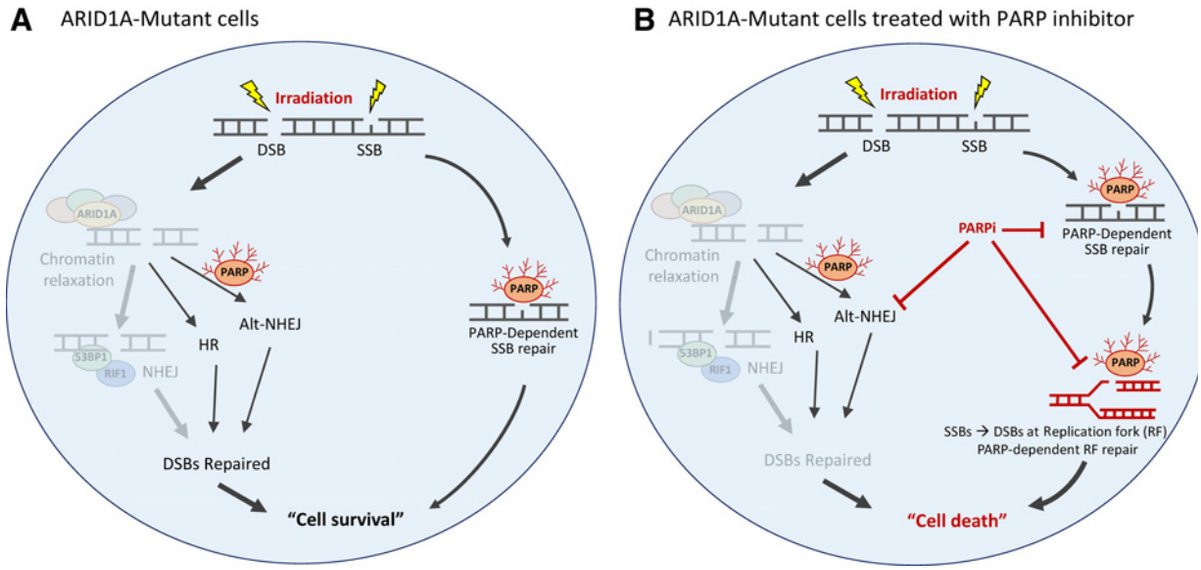

Figure 5.

ARID1A deficiency renders cells dependent on compensatory DNA repair pathways involving PARP for repairing radiation-induced DNA breaks. **A,** Schematic models of the DNA repair pathways in ARID1A-mutant cells following irradiation. **B,** ARID1A-mutated cells with irradiation and PARP inhibitor combined treatment.

and animal weights did not differ between different groups before treatment (Supplementary Fig. S8A and S8B). Strikingly, irradiation combined with PARP inhibitor completely prevented the growth of ARID1A$^{-/-}$ tumors, demonstrating superior efficacy over either treatment alone (Fig. 4B). In contrast, the addition of PARP inhibitor did not enhance the effect of irradiation on reducing growth of ARID1A$^{+/+}$ tumors, which continued to progress insidiously (Fig. 4B). Immunoblotting of tumor lysates confirmed ARID1A expression and depletion of PARylated proteins by olaparib (Supplementary Fig. S8C and S8D). To determine whether combination treatment led to long-lasting effects that persisted after treatment was terminated, we followed the animals that received combination therapy for 4 additional weeks after the final treatment. We found that ARID1A$^{+/+}$ tumors regrew quickly after cessation of therapy, whereas ARID1A$^{-/-}$ tumors continued to shrink (Fig. 4C).

To determine the generalizability of these findings, we evaluated the same treatment regimen in additional xenograft models: ovarian clear cell carcinoma cell lines (RMG-1 and TOV21G) and uterine endometrioid cancer cell lines (ECC1 and HEC151). ECC1 and RMG-1 are ARID1A wild-type and express ARID1A protein, while HEC151 and TOV21G lose expression of ARID1A due to inactivation mutations (right, Fig. 4A). In mice bearing ARID1A-expressing tumors (ECC1 and RMG-1), PARP inhibition did not confer additional antitumor benefits over irradiation, whereas combination therapy was more effective than irradiation or PARP inhibitor monotherapy in mice bearing ARID1A-deficient tumors (HEC151 or TOV21G; Fig. 4D). IHC staining for γH2AX and cleaved caspase-3 revealed significantly higher levels of DSBs and cell death in ARID1A-deficient tumors than in ARID1A-expressing tumors following combination treatment (Fig. 4E). We continued monitoring the mice for another 3 weeks after treatment. While long-term remissions were achieved in mice bearing ARID1A-deficient tumors (HEC151 and TOV21G), early recurrence and tumor regrowth was observed in mice with ARID1A-expressing tumors (Supplementary Fig. S8E).

Discussion

This investigation of mechanisms underlying the biological functions of ARID1A in NHEJ repair yielded novel biological and translational implications. Of particular importance, we discovered that combining radiation with PARP inhibitor therapy is highly effective in eradicating ARID1A-mutated tumors. The effect of PARP inhibition on ARID1A-mutated tumors is mechanistically distinct from effects on HR-deficient tumors, such as those harboring deleterious BRCA mutations, which are intrinsically sensitive to PARP inhibitor monotherapy due to their loss of ability to repair PARP inhibitor–induced replication fork collapse (34, 35). As to why PARP inhibitor monotherapy is less effective in ARID1A-deficient tumors, we speculate that the HR machinery in ARID1A-deficient cells remains intact, and the activity is sufficient to repair DSBs resulting from replication fork stalling, including those induced by PARP trapping.

NHEJ is the primary repair mechanism for ionizing radiation–induced DSBs and the repair is active at all stages of cell cycle including G_1 (36). We hypothesize that due to the reduced NHEJ repair capacity in ARID1A-deficient cells, radiation-induced DNA breaks are not effectively repaired. As a result, ARID1A-deficient cells depend on other PARP-dependent DNA repair systems including HR, alt-NHEJ, and replication fork repairs to maintain DNA integrity. Accordingly, ionizing radiation–induced DNA breaks cause ARID1A-deficient cells to become profoundly dependent on these PARP-dependent repair pathways, which renders them highly sensitive to PARP inhibitors (Fig. 5; ref. 35). If this hypothesis is correct, DNA-damaging agents that induce similar types of DNA breaks should exhibit synergy with PARP inhibition in ARID1A-mutated tumors, including human tumors. Indeed,

our unpublished data using the alkylating agent, temozolomide, supports this view.

A treatment regimen of combined ionizing radiation and PARP inhibition could, in principle, mediate effective killing of ARID1A-mutated tumor cells while sparing normal tissues, which retain ARID1A expression and functionality for efficient DNA repair. While the synthetic lethality of PARP inhibition in HR-defective BRCA-mutated ovarian carcinomas is well-documented, this study provides evidence in a new arena, demonstrating compromised DNA repair efficiency as an Achilles' heel in ARID1A-mutated malignancies.

Radiotherapy is often a consideration in the management of locally advanced and recurrent endometrial cancers, particularly for patients who are too frail for surgery (37, 38). The anatomic distribution of clear cell and endometrioid carcinomas, which are characteristically confined to the pelvis, but which may metastasize to lymph nodes, renders these tumor types amenable to radiotherapy. ARID1A loss, which occurs in a significant proportion of cases, also confers intrinsic sensitivity to radiation. Importantly, our preclinical data support enhancement of efficacy by the combination of fractionated radiation with PARP inhibition, and should be tested in late-stage, recurrent uterine endometrioid and clear cell carcinomas. With improvements in delivery of targeted radiation, there is renewed interest for applications of radiotherapy for ovarian cancer (39), and future studies should consider the addition of a PARP inhibitor to treat chemoresistant ovarian endometrioid and clear cell carcinomas.

Importantly, identifying molecular genetic alterations predicting clinical response to radiotherapy remains an unmet need. Future clinical trials to test the proposed combination treatment strategy might consider accruing patients based on ARID1A mutation status, with the intent to evaluate ARID1A mutation or inactivation as a potential biomarker for predicting treatment outcome. A relevant question to be addressed is whether tumors with mutations in other subunits of the ARID1A chromatin remodeling complex display a similar phenotype. Finally, efforts to optimize dosing schedules and safety monitoring will be necessary for translation of our preclinical findings to human trials.

Disclosure of Potential Conflicts of Interest

S. Gaillard is a consultant/advisory board member for AstraZeneca, Tesaro, Merck, and Immunogen. No potential conflicts of interest were disclosed by the other authors.

Authors' Contributions

Conception and design: Y. Park, M.H. Chui, M.A. Bellani, V.A. Bohr, I.-M. Shih, T.-L. Wang

Development of methodology: Y. Park, Y.S. Rahmanto, R.A. Shamanna, M.M. Seidman

Acquisition of data (provided animals, acquired and managed patients, provided facilities, etc.): Y. Park, Y.S. Rahmanto, Z.-C. Yu, R.A. Shamanna, M.A. Bellani, A. Ayhan

Analysis and interpretation of data (e.g., statistical analysis, biostatistics, computational analysis): Y. Park, M.H. Chui, Z.-C. Yu, R.A. Shamanna, A. Ayhan, S. Franco, V.A. Bohr, I.-M. Shih, T.-L. Wang

Writing, review, and/or revision of the manuscript: Y. Park, M.H. Chui, Z.-C. Yu, S. Gaillard, A. Ayhan, A. Viswanathan, M.M. Seidman, S. Franco, A. Leung, V.A. Bohr, I.-M. Shih, T.-L. Wang

Administrative, technical, or material support (i.e., reporting or organizing data, constructing databases): Y.S. Rahmanto, A. Ayhan, I.-M. Shih

Study supervision: A. Ayhan, S. Franco, A. Leung, T.-L. Wang

Acknowledgments

The authors thank Dr. Tae Magomi's contribution to the preliminary work. The study is supported by NIH/NCI R21CA165807, RO1CA129080, P50CA228991, RO1CA215483, Gray Foundation, and the Richard W. TeLinde Endowment Fund from the Department of Gynecology and Obstetrics, Johns Hopkins University (Baltimore, MD).

The costs of publication of this article were defrayed in part by the payment of page charges. This article must therefore be hereby marked *advertisement* in accordance with 18 U.S.C. Section 1734 solely to indicate this fact.

Received January 3, 2019; revised April 13, 2019; accepted June 10, 2019; published first June 13, 2019.

References

1. Wilson BG, Roberts CW. SWI/SNF nucleosome remodellers and cancer. Nat Rev Cancer 2011;11:481–92.
2. Jones S, Wang TL, Shih Ie M, Mao TL, Nakayama K, Roden R, et al. Frequent mutations of chromatin remodeling gene ARID1A in ovarian clear cell carcinoma. Science 2010;330:228–31.
3. Guan B, Wang TL, Shih Ie M. ARID1A, a factor that promotes formation of SWI/SNF-mediated chromatin remodeling, is a tumor suppressor in gynecologic cancers. Cancer Res 2011;71:6718–27.
4. Guan B, Mao TL, Panuganti PK, Kuhn E, Kurman RJ, Maeda D, et al. Mutation and loss of expression of ARID1A in uterine low-grade endometrioid carcinoma. Am J Surg Pathol 2011;35:625–32.
5. Wiegand KC, Shah SP, Al-Agha OM, Zhao Y, Tse K, Zeng T, et al. ARID1A mutations in endometriosis-associated ovarian carcinomas. N Engl J Med 2010;363:1532–43.
6. Cancer Genome Atlas Research Network, Kandoth C, Schultz N, Cherniack AD, Akbani R, Liu Y, et al. Integrated genomic characterization of endometrial carcinoma. Nature 2013;497:67–73.
7. Jones S, Stransky N, McCord CL, Cerami E, Lagowski J, Kelly D, et al. Genomic analyses of gynaecologic carcinosarcomas reveal frequent mutations in chromatin remodelling genes. Nat Commun 2014;5:5006.
8. Wu RC, Wang TL, Shih Ie M. The emerging roles of ARID1A in tumor suppression. Cancer Biol Ther 2014;15:655–64.
9. Bailey P, Chang DK, Nones K, Johns AL, Patch AM, Gingras MC, et al. Genomic analyses identify molecular subtypes of pancreatic cancer. Nature 2016;531:47–52.
10. Cancer Genome Atlas Research Network. Comprehensive molecular characterization of urothelial bladder carcinoma. Nature 2014;507:315–22.
11. Schulze K, Imbeaud S, Letouze E, Alexandrov LB, Calderaro J, Rebouissou S, et al. Exome sequencing of hepatocellular carcinomas identifies new mutational signatures and potential therapeutic targets. Nat Genet 2015;47:505–11.
12. Wang K, Kan J, Yuen ST, Shi ST, Chu KM, Law S, et al. Exome sequencing identifies frequent mutation of ARID1A in molecular subtypes of gastric cancer. Nat Genet 2011;43:1219–23.
13. Guan B, Rahmanto YS, Wu RC, Wang Y, Wang Z, Wang TL, et al. Roles of deletion of Arid1a, a tumor suppressor, in mouse ovarian tumorigenesis. J Nat Cancer Inst 2014;106: pii:dju146.
14. Chandler RL, Damrauer JS, Raab JR, Schisler JC, Wilkerson MD, Didion JP, et al. Coexistent ARID1A-PIK3CA mutations promote ovarian clear-cell tumorigenesis through pro-tumorigenic inflammatory cytokine signalling. Nat Commun 2015;6:6118.
15. Muller FL, Aquilanti EA, DePinho RA. Collateral lethality: a new therapeutic strategy in oncology. Trends Cancer 2015;1:161–73.
16. Dedes KJ, Wilkerson PM, Wetterskog D, Weigelt B, Ashworth A, Reis-Filho JS. Synthetic lethality of PARP inhibition in cancers lacking BRCA1 and BRCA2 mutations. Cell Cycle 2011;10:1192–9.
17. Fong PC, Boss DS, Yap TA, Tutt A, Wu P, Mergui-Roelvink M, et al. Inhibition of poly(ADP-ribose) polymerase in tumors from BRCA mutation carriers. N Engl J Med 2009;361:123–34.

18. Chai B, Huang J, Cairns BR, Laurent BC. Distinct roles for the RSC and Swi/Snf ATP-dependent chromatin remodelers in DNA double-strand break repair. Genes Develop 2005;19:1656–61.
19. Densham RM, Garvin AJ, Stone HR, Strachan J, Baldock RA, Daza-Martin M, et al. Human BRCA1-BARD1 ubiquitin ligase activity counteracts chromatin barriers to DNA resection. Nat Struct Mol Biol 2016;23:647–55.
20. Aydin OZ, Marteijn JA, Ribeiro-Silva C, Rodriguez Lopez A, Wijgers N, Smeenk G, et al. Human ISWI complexes are targeted by SMARCA5 ATPase and SLIDE domains to help resolve lesion-stalled transcription. Nucleic Acids Res 2014;42:8473–85.
21. Watanabe R, Ui A, Kanno S, Ogiwara H, Nagase T, Kohno T, et al. SWI/SNF factors required for cellular resistance to DNA damage include ARID1A and ARID1B and show interdependent protein stability. Cancer Res 2014;74:2465–75.
22. Shen J, Peng Y, Wei L, Zhang W, Yang L, Lan L, et al. ARID1A deficiency impairs the DNA damage checkpoint and sensitizes cells to PARP inhibitors. Cancer Disc 2015;5:752–67.
23. Lu H, Shamanna RA, de Freitas JK, Okur M, Khadka P, Kulikowicz T, et al. Cell cycle-dependent phosphorylation regulates RECQL4 pathway choice and ubiquitination in DNA double-strand break repair. Nat Commun 2017;8:2039.
24. Perets R, Wyant GA, Muto KW, Bijron JG, Poole BB, Chin KT, et al. Transformation of the fallopian tube secretory epithelium leads to high-grade serous ovarian cancer in Brca;Tp53;Pten models. Cancer Cell 2013;24:751–65.
25. Suryo Rahmanto Y, Jung JG, Wu RC, Kobayashi Y, Heaphy CM, Meeker AK, et al. Inactivating ARID1A tumor suppressor enhances TERT transcription and maintains telomere length in cancer cells. J Biol Chem 2016;291:9690–9.
26. Yu Y, Gaillard S, Phillip JM, Huang TC, Pinto SM, Tessarollo NG, et al. Inhibition of spleen tyrosine kinase potentiates paclitaxel-induced cytotoxicity in ovarian cancer cells by stabilizing microtubules. Cancer Cell 2015;28:82–96.
27. Chou TC. Drug combination studies and their synergy quantification using the Chou-Talalay method. Cancer Res 2010;70:440–6.
28. Certo MT, Ryu BY, Annis JE, Garibov M, Jarjour J, Rawlings DJ, et al. Tracking genome engineering outcome at individual DNA breakpoints. Nat Methods 2011;8:671–6.
29. Chiruvella KK, Liang Z, Wilson TE. Repair of double-strand breaks by end joining. Cold Spring Harb Perspect Biol 2013;5:a012757.
30. Howard SM, Yanez DA, Stark JM. DNA damage response factors from diverse pathways, including DNA crosslink repair, mediate alternative end joining. PLoS Genet 2015;11:e1004943.
31. Branzei D, Foiani M.Regulation of DNA repair throughout the cell cycle. Nat Rev Mol Cell Biol 2008;9:297–308.
32. Atagi S, Kawahara M, Yokoyama A, Okamoto H, Yamamoto N, Ohe Y, et al. Thoracic radiotherapy with or without daily low-dose carboplatin in elderly patients with non-small-cell lung cancer: a randomised, controlled, phase 3 trial by the Japan Clinical Oncology Group (JCOG0301). Lancet Oncol 2012;13:671–8.
33. Douple EB, Richmond RC, O'Hara JA, Coughlin CT. Carboplatin as a potentiator of radiation therapy. Cancer Treat Rev 1985;12:111–24.
34. Konecny GE, Kristeleit RS.PARP inhibitors for BRCA1/2-mutated and sporadic ovarian cancer: current practice and future directions. Br J Cancer 2016;115:1157–73.
35. Murai J, Huang SY, Das BB, Renaud A, Zhang Y, Doroshow JH, et al. Trapping of PARP1 and PARP2 by clinical PARP inhibitors. Cancer Res 2012;72:5588–99.
36. Mahaney BL, Meek K, Lees-Miller SP. Repair of ionizing radiation-induced DNA double-strand breaks by non-homologous end-joining. Biochem J 2009;417:639–50.
37. Suidan RS, He W, Sun CC, Zhao H, Smith GL, Klopp AH, et al. National trends, outcomes, and costs of radiation therapy in the management of low- and high-intermediate risk endometrial cancer. Gynecol Oncol 2019;152:439–44.
38. van der Steen-Banasik E, Christiaens M, Shash E, Coens C, Casado A, Herrera FG, et al. Systemic review: radiation therapy alone in medical non-operable endometrial carcinoma. Eur J Cancer 2016;65:172–81.
39. Fields EC, McGuire WP, Lin L, Temkin SM. Radiation treatment in women with ovarian cancer: past, present, and future. Front Oncol 2017;7:177.